Journal of Magnetism and Magnetic Materials 472 (2019) 49–52

Contents lists available at ScienceDirect

Journal of Magnetism and Magnetic Materials

journal homepage: www.elsevier.com/locate/jmmm

# Structure origin of abnormal magnetic behavior of Fe-P-C amorphous alloys

ARTICLE INFO

*Keywords:*
Amorphous alloy
Saturation magnetic flux density
Synchrotron X-ray diffraction

ABSTRACT

The magnetic properties of a series of Fe-P-C amorphous alloys were investigated. $Fe_{80}P_{13}C_7$ shows the largest saturation magnetic flux density among all the $Fe_{80}P_{20-x}C_x$ ($x$ = 7–9) alloys, which is supported by the hyperfine field distribution. Synchrotron X-ray diffraction was performed to explore the underlying structure mechanism. It is found that $Fe_{80}P_{13}C_7$ amorphous alloy has a larger atomic volume accompanied by a larger first peak position value of the reduced pair distribution function compared with those of $Fe_{80}P_{12}C_8$ and $Fe_{80}P_{11}C_9$. The origin of the unusual magnetic behavior of $Fe_{80}P_{13}C_7$ is thought to be the large Fe-Fe bond length.

## 1. Introduction

Fe-based amorphous alloy (AA), a promising soft magnetic material, has attracted vast of interests [1,2]. Compared with silicon steels, one major shortcoming of Fe-based AAs is their relative low saturation magnetic flux density ($B_S$). Numerous works have been done to improve the $B_S$ for Fe-based AAs. Li et al. [3] developed a Fe-based AA with a high $B_S$ of 1.65 T by composition design. Extremely high $B_S$ of 1.86 T [4] and even 1.92 T [5] for Fe-Co-based AAs were obtained after a controlled annealing. Among these investigations, it was found that the $Fe_{80}P_{11}C_9$ glassy sample has a $B_S$ of 1.37 T [6], while the $B_S$ for $Fe_{80}P_{13}C_7$ is 1.53 T [7]. Such huge difference in $B_S$ seems implausible, since the concentration of Fe dominating the magnetization in these two alloys is the same.

In principle, the average magnetic moment $\mu_{av}$ of 3*d*-transitional-metal-based alloys results from unpaired electron spins [8]. Accordingly, $\mu_{av}$ may be simply written as: $\mu_{av} = [2(N_{sp}^{\uparrow} + N_d^{\uparrow}) - Z_{av}]\cdot\mu_B$, where $N_{sp}^{\uparrow}$ and $N_d^{\uparrow}$ are the up-spin electron numbers of *sp* and *d* band components, $\mu_B$ is Bohr magnetron and $Z_{av}$ donates the average electronic valence. Therefore, $\mu_{av}$ can be easily deduced assuming $N_{sp}^{\uparrow}$ and $N_d^{\uparrow}$ are constant under alloying. However, this assumption itself seems too tremendous to obscure. On the one hand, Malozemoff et al. [9] put forward "band-gap theory" to describe $\mu_{av}$ for strong ferromagnetism and demonstrated that the constancy of $N_{sp}^{\uparrow}$ is debated. On the other hand, Fe-based AAs is generally weak ferromagnetism with a partially empty spin-up *d* band, which has been verified by several groups via computational simulation [10,11], so that the $\mu_{av}$ for Fe-based AAs is extremely sensitive to the changes in Fe-Fe exchange interaction. Recently, Liu et al. [12] proposed a set of simple rules to calculate the $B_S$ and declared that the deviation between calculated and experimental values may be caused by the formation of densely packed Fe local structures. In short, the $B_S$ of Fe-based AAs is local structure dependent. Aiming at investigating the structure origin of the $B_S$ difference between $Fe_{80}P_{11}C_9$ and $Fe_{80}P_{13}C_7$ AAs, synchrotron X-ray diffraction is performed. Other three Fe-P-C AAs $Fe_{78}P_{14}C_8$, $Fe_{80}P_{12}C_8$ and $Fe_{82}P_{12}C_6$ are also studied for comparison.

## 2. Materials and methods

Fe-P-C alloy ingots were prepared by high vacuum arc-melting and they were remelted at least four times under a Ti-gettered argon atmosphere to ensure the chemical homogeneity. Ribbons with a thickness of about 25 μm were then produced by single roller spinning method. The amorphous structure of all samples was then confirmed by X-ray diffraction with Cu Kα radiation and the composition analysis was conducted by energy-dispersive spectroscopy (EDS) equipped in a field emission-scanning electron microscope. Magnetic properties of the ribbons with a length of 30 mm and width of ~2 mm were measured using a DC *B*–*H* loop tracer. $^{57}$Fe Mössbauer spectra were collected with $^{57}$Co(Rh) as γ-ray source in transmission geometry. Normos software was applied to fit Mössbauer spectra and we defined the range of the magnetic hyperfine field ($B_{hf}$) from 0 T to 38 T with a step size of 1 T. The calibration of Mössbauer spectra was carried out using an α-Fe foil. Synchrotron X-ray diffraction with a wavelength of 0.1173 Å was carried out at the beamline 11-ID-C in Advanced Photon Source, Argonne National Laboratory. The diffraction data were normalized by software PDFgetX2 to get the structure factors $S(Q)$ and the corresponding reduced pair distribution functions PDFs $G(r)$.

## 3. Results and discussion

Fig. 1(a) shows the XRD patterns for as-spun Fe-P-C alloy ribbons. All the patterns exhibit a typical broad halo without any discernible crystalline peak indicating the formation of amorphous structure. To detect the possible composition variation induced by the arc-melting, EDS analyses are conducted as shown in Fig. 1(b) and the atomic percent for each element are listed in Table 1. As can be seen, the experimental values for all the elements are very close to their corresponding nominal composition except for the slight enlargement of C rising from the free carbon in the air. Therefore, the volatilization of elements can be neglected and we use the nominal composition in the following for simplicity.

Fig. 2(a) shows the hysteresis loops of as-spun Fe-P-C ribbons. The $B_S$ for $Fe_{78}P_{14}C_8$, $Fe_{80}P_{11}C_9$, $Fe_{80}P_{12}C_8$, $Fe_{80}P_{13}C_7$ and $Fe_{82}P_{12}C_6$ are 1.31, 1.37, 1.42, 1.51 and 1.56 T, respectively. These values agree well

https://doi.org/10.1016/j.jmmm.2018.10.001
Received 3 August 2018; Received in revised form 12 September 2018; Accepted 1 October 2018
Available online 03 October 2018
0304-8853/ 

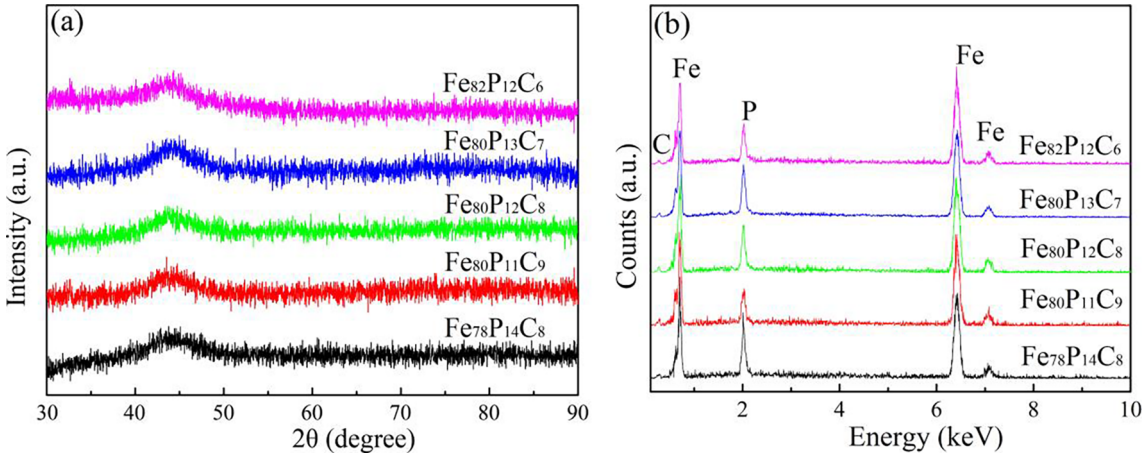


**Fig. 1.** XRD patterns (a) and EDS analyses (b) for Fe-P-C alloy ribbons.

**Table 1**
Average chemical composition of as-spun Fe-P-C alloy ribbons deduced from the EDS analyses.

| Nominal composition | Fe (at. %) | P (at. %) | C (at. %) |
|---|---|---|---|
| $Fe_{78}P_{14}C_8$ | 77.80 | 13.15 | 9.05 |
| $Fe_{80}P_{11}C_9$ | 79.54 | 10.06 | 10.40 |
| $Fe_{80}P_{12}C_8$ | 79.37 | 11.41 | 9.22 |
| $Fe_{80}P_{13}C_7$ | 79.34 | 12.44 | 8.22 |
| $Fe_{82}P_{12}C_6$ | 81.68 | 11.75 | 6.57 |

with the literature [6,7]. The enlargement of the $B_S$ with the increase of Fe is merited as the magnetization mainly originates from Fe. According to the related work [12], $B_S$ can be expressed as $B_S = N_A\mu_{av}\mu_B/V_m$, where $N_A$ and $V_m$ are the Avogadro number and the molar volume of the alloy. In the present work, the concentration of Fe is about 80%, we may take $V_m \approx V_{m,Fe} = 7.092 * 10^{-6}\,m^3$ as an approximation. Thus, $\mu_{av}$ can be calculated by the relation: $\mu_{av} = V_{m,Fe}B_S/(N_A\mu_B)$. Williams et al. [13] proposed a generalized Slater-Pauling plot of $\mu_{av}$ versus average magnetic valence $Z_{m,av} = \Sigma x_i {Z_m}^i$, where $x$ is the atom fraction and ${Z_m}^i = 2N_{di}{}^{\uparrow} - Z^i$ is the magnetic valence ($Z^i$ being the electronic valence) of $i$th constituent. If $i$ is a metalloid, $2N_{di}{}^{\uparrow} = 0$ and Fe has $2N_{di}{}^{\uparrow} = 10$. The generalized Slater-Pauling plot for several typical Fe-P-C AAs with a part of data from the literature [14,15] is illustrated in Fig. 2(b). One can find a positive correlation between the average magnetic moment $\mu_{av}$ and the average magnetic valence $Z_{m,av}$, but small deviation does exist. Note that the slope of lines is about 1.65, larger than the theoretic value of 1. The reason lies in the fact that magnetic valence theory roots in the rigid-band model, which is too simple to give a satisfactory explanation for the $\mu_{av}$. That is to say that the magnetic behavior of the investigated Fe-P-C AAs cannot be simply explained by the magnetic valence theory and the reason why $Fe_{80}P_{13}C_7$ AA has the largest $B_S$ among all the $Fe_{80}P_{20-x}C_x$ ($x$ = 7–9) alloys is still far from understood. Interestingly, all these alloys can be divided into two groups lying in two parallel lines. The origin for this phenomenon is not clear now and the difference in $N_{sp}{}^{\uparrow}$ may make a contribution.

$^{57}$Fe Mössbauer spectra are collected to provide more information about the Fe-P-C AAs. The typical broaden sextet lines in Fig. 3(a) again confirm the amorphous structure of the as-spun Fe-P-C ribbons. Magnetic hyperfine field distributions $P(B_{hf})$ of these alloy ribbons are shown in Fig. 3(b) where all the patterns consist two distinct, separated humps. The occurrence of the small hump is widely observed in Fe-based AAs and is often suggested to be caused by the existence of the nonmagnetic elements in the vicinity of Fe reducing the magnetic interaction between Fe atoms [16,17]. The $P(B_{hf})$ patterns of the samples move towards the right with the increase of Fe. When Fe content is constantly 80%, the high-field hump shifts to larger values of $B_{hf}$ with more P replacing C. By comparison, the $B_S$ of the alloys can be ordered as: $Fe_{78}P_{14}C_8$ < $Fe_{80}P_{11}C_9$ < $Fe_{80}P_{12}C_8$ < $Fe_{80}P_{13}C_7$ < $Fe_{82}P_{12}C_6$ in magnitude, because average hyperfine field values are someway proportional to $B_S$. This agrees well with the results obtained from the DC $B$–$H$ loop tracer.

To seek the structure origin of the large $B_S$ of $Fe_{80}P_{13}C_7$ AA, synchrotron X-ray diffraction is performed. Profiles of the structure factors $S(Q)$ of the Fe-P-C ribbons are shown in Fig. 4(a). All the samples are amorphous, and no sharp peaks can be observed on the $S(Q)$ patterns as expected. The first peak positions $Q_1$ were obtained by fitting the peak using a pseudo-Voigt function and $Q_1$ for the investigated alloys are present in Fig. 4(b). One can see that $Q_1$ moves towards large values with the increase of Fe. Such behavior has also been observed in Co-FeSiB AAs by substituting Si with Fe [18]. Moreover, $Q_1$ for $Fe_{80}P_{11}C_9$ and $Fe_{80}P_{12}C_8$ are similar, while $Fe_{80}P_{13}C_7$ shows an anomaly possessing a relative small $Q_1$. It has been reported a power-law scaling of $Q_1$ with the atomic volume [19]. Therefore, the abnormally small value of $Q_1$ clearly evidences the atomic volume expansion in $Fe_{80}P_{13}C_7$ AA.

A further detailed study on the structure of Fe-P-C AAs was conducted in real space. Fig. 5(a) shows reduced PDFs $G(r)$ of the Fe-P-C ribbons. Positions and full width at half maximum (FWHM) of first $G(r)$ peak obtained from Gaussian fits are illustrated in Fig. 5(b). Consistent with the results of $S(Q)$, $r_1$ shows a reduction with Fe content increasing. Again, an anomaly that the first $G(r)$ peak locates at a relatively large position value of $r$ arises for $Fe_{80}P_{13}C_7$ AA. Taking into account the values of the X-ray weighting factor (0.787, 0.819, 0.812, 0.806, 0.824 for the five investigated alloys, respectively), the dominant atomic pair is Fe-Fe. Since $G(r)$ peaks, to some extent, reflect the distance between atoms in different atomic shells, the above results manifest that the $Fe_{80}P_{13}C_7$ AA has a large average Fe-Fe bond length. Furthermore, the change in FWHM is similar with that of $r_1$ but with a larger error, which indicates the occurrence of the correlation length variation in the investigated Fe-P-C alloys. As mentioned in the introduction, $\mu_{av}$ of Fe-based AAs is sensitive to the local structure. It is known that interatomic distance between neighboring Fe atoms in Fe-based AAs is smaller than the optimal value for the largest exchange interacting strength $I_{ex}$. The increase in Fe-Fe bond length would result in $I_{ex}$ enhancement and thus $\mu_{av}$ enlargement. Therefore, the unusually large $B_S$ for $Fe_{80}P_{13}C_7$ alloy can be attributed to its relatively large atomic distance.

Having a high $B_S$ is desired for Fe-based AA. The most common and easiest strategy is increasing the Fe content. But it will inevitably lead to the deterioration of the glass forming ability. Here, we show that the relatively high $B_S$ of $Fe_{80}P_{13}C_7$ is the consequence of its large Fe-Fe bond length. In addition, recent works has confirmed that Fe magnetic moment is indeed bond length dependent by *ab initio* molecular